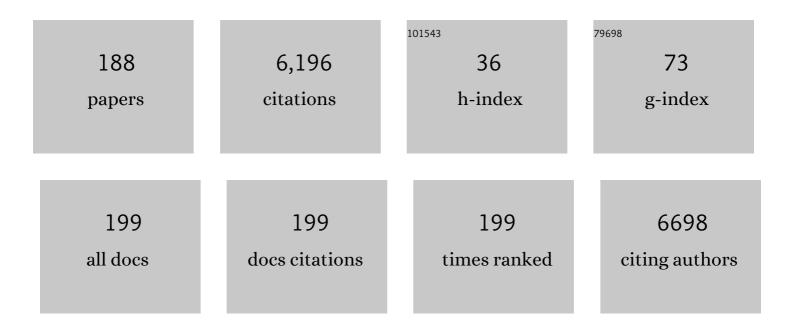
Julia A Schnabel

List of Publications by Year in descending order

Source: https://exaly.com/author-pdf/529827/publications.pdf Version: 2024-02-01



ILLIA A SCHNAREL

#	Article	IF	CITATIONS
1	MIND: Modality independent neighbourhood descriptor for multi-modal deformable registration. Medical Image Analysis, 2012, 16, 1423-1435.	11.6	478
2	Evaluation of Registration Methods on Thoracic CT: The EMPIRE10 Challenge. IEEE Transactions on Medical Imaging, 2011, 30, 1901-1920.	8.9	363
3	Automatic construction of 3-D statistical deformation models of the brain using nonrigid registration. IEEE Transactions on Medical Imaging, 2003, 22, 1014-1025.	8.9	350
4	Automatic construction of multiple-object three-dimensional statistical shape models: application to cardiac modeling. IEEE Transactions on Medical Imaging, 2002, 21, 1151-1166.	8.9	325
5	Reconstruction of fetal brain MRI with intensity matching and complete outlier removal. Medical Image Analysis, 2012, 16, 1550-1564.	11.6	301
6	Validation of nonrigid image registration using finite-element methods: application to breast MR images. IEEE Transactions on Medical Imaging, 2003, 22, 238-247.	8.9	224
7	MRF-Based Deformable Registration and Ventilation Estimation of Lung CT. IEEE Transactions on Medical Imaging, 2013, 32, 1239-1248.	8.9	208
8	A Generic Framework for Non-rigid Registration Based on Non-uniform Multi-level Free-Form Deformations. Lecture Notes in Computer Science, 2001, , 573-581.	1.3	185
9	An evaluation of four automatic methods of segmenting the subcortical structures in the brain. NeuroImage, 2009, 47, 1435-1447.	4.2	180
10	Breast Image Analysis for Risk Assessment, Detection, Diagnosis, and Treatment of Cancer. Annual Review of Biomedical Engineering, 2013, 15, 327-357.	12.3	175
11	Objective assessment of deformable image registration in radiotherapy: A multiâ€institution study. Medical Physics, 2008, 35, 5944-5953.	3.0	132
12	Deep Learning for PET Image Reconstruction. IEEE Transactions on Radiation and Plasma Medical Sciences, 2021, 5, 1-25.	3.7	128
13	Nonlinear smoothing for reduction of systematic and random errors in diffusion tensor imaging. Journal of Magnetic Resonance Imaging, 2000, 11, 702-710.	3.4	116
14	Fully Automated, Quality-Controlled Cardiac Analysis From CMR. JACC: Cardiovascular Imaging, 2020, 13, 684-695.	5.3	113
15	Towards Realtime Multimodal Fusion for Image-Guided Interventions Using Self-similarities. Lecture Notes in Computer Science, 2013, 16, 187-194.	1.3	104
16	Factors influencing the accuracy of biomechanical breast models. Medical Physics, 2006, 33, 1758-1769.	3.0	98
17	Registration-Based Interpolation. IEEE Transactions on Medical Imaging, 2004, 23, 922-926.	8.9	87
18	Evaluation of automatic neonatal brain segmentation algorithms: The NeoBrainS12 challenge. Medical Image Analysis, 2015, 20, 135-151.	11.6	85

#	Article	IF	CITATIONS
19	Automatic CNN-based detection of cardiac MR motion artefacts using k-space data augmentation and curriculum learning. Medical Image Analysis, 2019, 55, 136-147.	11.6	71
20	An implicit sliding-motion preserving regularisation via bilateral filtering for deformable image registration. Medical Image Analysis, 2014, 18, 1299-1311.	11.6	69
21	Piecewise-diffeomorphic image registration: Application to the motion estimation between 3D CT lung images with sliding conditions. Medical Image Analysis, 2013, 17, 182-193.	11.6	68
22	Left-Ventricle Quantification Using Residual U-Net. Lecture Notes in Computer Science, 2019, , 371-380.	1.3	65
23	Probabilistic inference of regularisation in non-rigid registration. Neurolmage, 2012, 59, 2438-2451.	4.2	59
24	Deformable image registration by combining uncertainty estimates from supervoxel belief propagation. Medical Image Analysis, 2016, 27, 57-71.	11.6	58
25	A level-set approach to joint image segmentation and registration with application to CT lung imaging. Computerized Medical Imaging and Graphics, 2018, 65, 58-68.	5.8	53
26	Automatic 3D ASM Construction via Atlas-Based Landmarking and Volumetric Elastic Registration. Lecture Notes in Computer Science, 2001, , 78-91.	1.3	51
27	Advances and challenges in deformable image registration: From image fusion to complex motion modelling. Medical Image Analysis, 2016, 33, 145-148.	11.6	50
28	Deep Learning-Based Detection and Correction of Cardiac MR Motion Artefacts During Reconstruction for High-Quality Segmentation. IEEE Transactions on Medical Imaging, 2020, 39, 4001-4010.	8.9	49
29	Virtual interaction and visualisation of 3D medical imaging data with VTK and Unity. Healthcare Technology Letters, 2018, 5, 148-153.	3.3	48
30	BESNet: Boundary-Enhanced Segmentation of Cells in Histopathological Images. Lecture Notes in Computer Science, 2018, , 228-236.	1.3	46
31	Evaluation of 2D and 3D ultrasound tracking algorithms and impact on ultrasoundâ€guided liver radiotherapy margins. Medical Physics, 2018, 45, 4986-5003.	3.0	43
32	Evaluation of MRI to Ultrasound Registration Methods for Brain Shift Correction: The CuRIOUS2018 Challenge. IEEE Transactions on Medical Imaging, 2020, 39, 777-786.	8.9	42
33	An objective comparison of detection and segmentation algorithms for artefacts in clinical endoscopy. Scientific Reports, 2020, 10, 2748.	3.3	41
34	Comparison and Evaluation of Segmentation Techniques for Subcortical Structures in Brain MRI. Lecture Notes in Computer Science, 2008, 11, 409-416.	1.3	40
35	Explicit Topological Priors for Deep-Learning Based Image Segmentation Using Persistent Homology. Lecture Notes in Computer Science, 2019, , 16-28.	1.3	39
36	Weakly Supervised Estimation of Shadow Confidence Maps in Fetal Ultrasound Imaging. IEEE Transactions on Medical Imaging, 2019, 38, 2755-2767.	8.9	38

#	Article	IF	CITATIONS
37	Hybrid Feature-Based Diffeomorphic Registration for Tumor Tracking in 2-D Liver Ultrasound Images. IEEE Transactions on Medical Imaging, 2013, 32, 1647-1656.	8.9	37
38	A DCE-MRI Driven 3-D Reaction-Diffusion Model of Solid Tumor Growth. IEEE Transactions on Medical Imaging, 2018, 37, 724-732.	8.9	37
39	Quantification of small cerebral ventricular volume changes in treated growth hormone patients using nonrigid registration. IEEE Transactions on Medical Imaging, 2002, 21, 1292-1301.	8.9	36
40	Quantitative evaluation of free-form deformation registration for dynamic contrast-enhanced MR mammography. Medical Physics, 2007, 34, 1221-1233.	3.0	36
41	A New Validation Method for X-ray Mammogram Registration Algorithms Using a Projection Model of Breast X-ray Compression. IEEE Transactions on Medical Imaging, 2007, 26, 1190-1200.	8.9	34
42	Validation of Non-rigid Registration Using Finite Element Methods. Lecture Notes in Computer Science, 2001, , 344-357.	1.3	34
43	Phenomenological Model of Diffuse Global and Regional Atrophy Using Finite-Element Methods. IEEE Transactions on Medical Imaging, 2006, 25, 1417-1430.	8.9	32
44	Accuracy assessment of global and local atrophy measurement techniques with realistic simulated longitudinal Alzheimer's disease images. NeuroImage, 2008, 42, 696-709.	4.2	32
45	A multi-scale variational neural network for accelerating motion-compensated whole-heart 3D coronary MR angiography. Magnetic Resonance Imaging, 2020, 70, 155-167.	1.8	32
46	AtrialJSQnet: A New framework for joint segmentation and quantification of left atrium and scars incorporating spatial and shape information. Medical Image Analysis, 2022, 76, 102303.	11.6	31
47	Clinical Trial of Oral Nelfinavir before and during Radiation Therapy for Advanced Rectal Cancer. Clinical Cancer Research, 2016, 22, 1922-1931.	7.0	30
48	Model-Based and Data-Driven Strategies in Medical Image Computing. Proceedings of the IEEE, 2020, 108, 110-124.	21.3	30
49	Registration of 3D fetal neurosonography and MRI. Medical Image Analysis, 2013, 17, 1137-1150.	11.6	29
50	Motion Correction and Parameter Estimation in dceMRI Sequences: Application to Colorectal Cancer. Lecture Notes in Computer Science, 2011, 14, 476-483.	1.3	28
51	Globally Optimal Deformable Registration on a Minimum Spanning Tree Using Dense Displacement Sampling. Lecture Notes in Computer Science, 2012, 15, 115-122.	1.3	28
52	Regional Multi-View Learning for Cardiac Motion Analysis: Application to Identification of Dilated Cardiomyopathy Patients. IEEE Transactions on Biomedical Engineering, 2019, 66, 956-966.	4.2	27
53	Global and Local Interpretability for Cardiac MRI Classification. Lecture Notes in Computer Science, 2019, , 656-664.	1.3	27
54	Medical image analysis on left atrial LGE MRI for atrial fibrillation studies: A review. Medical Image Analysis, 2022, 77, 102360.	11.6	27

#	Article	IF	CITATIONS
55	Correction of misaligned slices in multi-slice cardiovascular magnetic resonance using slice-to-volume registration. Journal of Cardiovascular Magnetic Resonance, 2008, 10, 13.	3.3	26
56	A landmark-free morphometrics pipeline for high-resolution phenotyping: application to a mouse model of Down syndrome. Development (Cambridge), 2021, 148, .	2.5	26
57	Non-parametric Discrete Registration with Convex Optimisation. Lecture Notes in Computer Science, 2014, , 51-61.	1.3	26
58	Comparison of biomechanical breast models: a case study. , 2002, , .		24
59	Breast Image Registration by Combining Finite Elements and Free-Form Deformations. Lecture Notes in Computer Science, 2010, , 736-743.	1.3	24
60	Longitudinal Brain MRI Analysis with Uncertain Registration. Lecture Notes in Computer Science, 2011, 14, 647-654.	1.3	23
61	Medical Image Registration. Biological and Medical Physics Series, 2010, , 131-154.	0.4	22
62	Probabilistic non-linear registration with spatially adaptive regularisation. Medical Image Analysis, 2015, 26, 203-216.	11.6	22
63	Segmentation of Vasculature From Fluorescently Labeled Endothelial Cells in Multi-Photon Microscopy Images. IEEE Transactions on Medical Imaging, 2019, 38, 1-10.	8.9	22
64	Non-local Shape Descriptor: A New Similarity Metric for Deformable Multi-modal Registration. Lecture Notes in Computer Science, 2011, 14, 541-548.	1.3	22
65	Virtual reality three-dimensional echocardiographic imaging for planning surgical atrioventricular valve repair. JTCVS Techniques, 2021, 7, 269-277.	0.4	21
66	Pieces-of-parts for supervoxel segmentation with global context: Application to DCE-MRI tumour delineation. Medical Image Analysis, 2016, 32, 69-83.	11.6	20
67	Ensemble Learning Incorporating Uncertain Registration. IEEE Transactions on Medical Imaging, 2013, 32, 748-756.	8.9	19
68	Fully automated myocardial strain estimation from cine MRI using convolutional neural networks. , 2018, , .		19
69	Automated Colorectal Tumour Segmentation in DCE-MRI Using Supervoxel Neighbourhood Contrast Characteristics. Lecture Notes in Computer Science, 2014, 17, 609-616.	1.3	18
70	Cardiac MR Motion Artefact Correction from K-space Using Deep Learning-Based Reconstruction. Lecture Notes in Computer Science, 2018, , 21-29.	1.3	18
71	Magnetic Resonance Fingerprinting Using Recurrent Neural Networks. , 2019, , .		18
72	Classification of amyloid status using machine learning with histograms of oriented 3D gradients. NeuroImage: Clinical, 2016, 12, 990-1003.	2.7	16

#	Article	IF	CITATIONS
73	Detection and Correction of Cardiac MRI Motion Artefacts During Reconstruction from k-space. Lecture Notes in Computer Science, 2019, , 695-703.	1.3	16
74	Exploring a new paradigm for the fetal anomaly ultrasound scan: Artificial intelligence in real time. Prenatal Diagnosis, 2022, 42, 49-59.	2.3	16
75	Myocardial Delineation via Registration in a Polar Coordinate System. Lecture Notes in Computer Science, 2002, , 651-658.	1.3	15
76	Myocardial delineation via registration in a polar coordinate system1. Academic Radiology, 2003, 10, 1349-1358.	2.5	15
77	Consistency of parametric registration in serial MRI studies of brain tumor progression. International Journal of Computer Assisted Radiology and Surgery, 2008, 3, 201-211.	2.8	15
78	Segmentation of the bladder wall using coupled level set methods. , 2011, , .		15
79	Revisiting overlap invariance in medical image alignment. , 2008, , .		14
80	Functional Parameters Derived from Magnetic Resonance Imaging Reflect Vascular Morphology in Preclinical Tumors and in Human Liver Metastases. Clinical Cancer Research, 2018, 24, 4694-4704.	7.0	14
81	Quantitative assessment of myelination patterns in preterm neonates using T2-weighted MRI. Scientific Reports, 2019, 9, 12938.	3.3	14
82	Multi-view Image Reconstruction: Application to Fetal Ultrasound Compounding. Lecture Notes in Computer Science, 2018, , 107-116.	1.3	14
83	Toward physiologically motivated registration of diagnostic CT and PET/CT of lung volumes. Medical Physics, 2013, 40, 021903.	3.0	13
84	Comparison of linear and nonlinear implementation of the compartmental tissue uptake model for dynamic contrast-enhanced MRI. Magnetic Resonance in Medicine, 2017, 77, 2414-2423.	3.0	13
85	Deep Learning Using K-Space Based Data Augmentation for Automated Cardiac MR Motion Artefact Detection. Lecture Notes in Computer Science, 2018, , 250-258.	1.3	13
86	LSTM Spatial Co-transformer Networks for Registration of 3D Fetal US and MR Brain Images. Lecture Notes in Computer Science, 2018, , 149-159.	1.3	13
87	Spatio-temporal pharmacokinetic model based registration of 4D PET neuroimaging data. NeuroImage, 2014, 84, 225-235.	4.2	12
88	Dense volumetric detection and segmentation of mediastinal lymph nodes in chest CT images. , 2018, , .		12
89	<title>Multiscale shape description of MR brain images using active contour models</title> . , 1996, , .		11
90	Hybrid feature-based Log-Demons registration for tumour tracking in 2-D liver ultrasound images. , 2012, , .		11

6

#	Article	IF	CITATIONS
91	Impact of image-based motion correction on dopamine D3/D2 receptor occupancy—comparison of groupwise and frame-by-frame registration approaches. EJNMMI Physics, 2015, 2, 15.	2.7	11
92	Quantifying Small Changes in Brain Ventricular Volume Using Non-rigid Registration. Lecture Notes in Computer Science, 2001, , 49-56.	1.3	11
93	Towards Whole Placenta Segmentation at Late Gestation Using Multi-view Ultrasound Images. Lecture Notes in Computer Science, 2019, , 628-636.	1.3	11
94	Edge- and Detail-Preserving Sparse Image Representations for Deformable Registration of Chest MRI and CT Volumes. Lecture Notes in Computer Science, 2013, 23, 463-474.	1.3	11
95	A Bayesian Approach for Spatially Adaptive Regularisation in Non-rigid Registration. Lecture Notes in Computer Science, 2013, 16, 10-18.	1.3	11
96	Active shape focusing. Image and Vision Computing, 1999, 17, 419-428.	4.5	10
97	MRI-Guided Motion-Corrected PET Image Reconstruction for Cardiac PET/MRI. Journal of Nuclear Medicine, 2021, 62, 1768-1774.	5.0	10
98	Oncological image analysis. Medical Image Analysis, 2016, 33, 7-12.	11.6	9
99	A Virtual Reality System for Improved Image-Based Planning of Complex Cardiac Procedures. Journal of Imaging, 2021, 7, 151.	3.0	9
100	Memory-Efficient Training for Fully Unrolled Deep Learned PET Image Reconstruction With Iteration-Dependent Targets. IEEE Transactions on Radiation and Plasma Medical Sciences, 2022, 6, 552-563.	3.7	9
101	Complex Lung Motion Estimation via Adaptive Bilateral Filtering of the Deformation Field. Lecture Notes in Computer Science, 2013, 16, 25-32.	1.3	9
102	Towards a more realistic biomechanical modelling of breast malignant tumours. Physics in Medicine and Biology, 2012, 57, 631-648.	3.0	8
103	Liver Motion Estimation via Locally Adaptive Over-Segmentation Regularization. Lecture Notes in Computer Science, 2015, , 427-434.	1.3	8
104	Registration of 3D Fetal Brain US and MRI. Lecture Notes in Computer Science, 2012, 15, 667-674.	1.3	8
105	Supervoxels for graph cuts-based deformable image registration using guided image filtering. Journal of Electronic Imaging, 2017, 26, 1.	0.9	8
106	GIFTed Demons: deformable image registration with local structure-preserving regularization using supervoxels for liver applications. Journal of Medical Imaging, 2018, 5, 1.	1.5	8
107	A Multi-task Approach Using Positional Information for Ultrasound Placenta Segmentation. Lecture Notes in Computer Science, 2020, , 264-273.	1.3	8
108	Registration and Segmentation in Medical Imaging. Studies in Computational Intelligence, 2014, , 137-156.	0.9	7

#	Article	IF	CITATIONS
109	Weakly Supervised Localisation for Fetal Ultrasound Images. Lecture Notes in Computer Science, 2018, , 192-200.	1.3	7
110	Virtual linear measurement system for accurate quantification of medical images. Healthcare Technology Letters, 2019, 6, 220-225.	3.3	7
111	Rigid Registration of Untracked Freehand 2D Ultrasound Sweeps to 3D CT of Liver Tumours. Lecture Notes in Computer Science, 2013, , 155-164.	1.3	7
112	Automated mediastinal lymph node detection from CT volumes based on intensity targeted radial structure tensor analysis. Journal of Medical Imaging, 2017, 4, 1.	1.5	7
113	Multispectral Image Registration Based on Local Canonical Correlation Analysis. Lecture Notes in Computer Science, 2014, 17, 202-209.	1.3	7
114	Image Reconstruction in a Manifold of Image Patches: Application to Whole-Fetus Ultrasound Imaging. Lecture Notes in Computer Science, 2019, , 226-235.	1.3	7
115	Classification of clusters of microcalcifications in digital breast tomosynthesis. , 2010, 2010, 3166-9.		6
116	Regional Differences in End-Diastolic Volumes between 3D Echo and CMR in HLHS Patients. Frontiers in Pediatrics, 2016, 4, 133.	1.9	6
117	Automatic Shadow Detection in 2D Ultrasound Images. Lecture Notes in Computer Science, 2018, , 66-75.	1.3	6
118	Fast Registration of 3D Fetal Ultrasound Images Using Learned Corresponding Salient Points. Lecture Notes in Computer Science, 2017, , 33-41.	1.3	6
119	Slice-to-volume registration using mutual information between probabilistic image classifications. , 2004, 5370, 1120.		5
120	Overlap invariance of cumulative residual entropy measures for multimodal image alignment. Proceedings of SPIE, 2009, , .	0.8	5
121	Fusion of perpendicular anisotropic MRI sequences. , 2011, , .		5
122	Piecewise-diffeomorphic registration of 3D CT/MR pulmonary images with sliding conditions. , 2012, , .		5
123	Textural mutual information based on cluster trees for multimodal deformable registration. , 2012, , .		5
124	Automatic left ventricular outflow tract classification for accurate cardiac MR planning. , 2018, , .		5
125	Patch-based lung ventilation estimation using multi-layer supervoxels. Computerized Medical Imaging and Graphics, 2019, 74, 49-60.	5.8	5
126	Automated CNN-Based Reconstruction of Short-Axis Cardiac MR Sequence from Real-Time Image Data. Lecture Notes in Computer Science, 2018, , 32-41.	1.3	5

#	Article	IF	CITATIONS
127	Synthesising Images and Labels Between MR Sequence Types with CycleGAN. Lecture Notes in Computer Science, 2019, , 45-53.	1.3	5
128	A New Similarity Metric for Groupwise Registration of Variable Flip Angle Sequences for Improved T 10 Estimation in DCE-MRI. Lecture Notes in Computer Science, 2014, , 154-163.	1.3	5
129	Tumour subregion analysis of colorectal liver metastases using semi-automated clustering based on DCE-MRI: Comparison with histological subregions and impact on pharmacokinetic parameter analysis. European Journal of Radiology, 2020, 126, 108934.	2.6	5
130	Accuracy Assessment of Global and Local Atrophy Measurement Techniques with Realistic Simulated Longitudinal Data. , 2007, 10, 785-792.		5
131	Syn-Net for Synergistic Deep-Learned PET-MR Reconstruction. , 2020, , .		5
132	Finite-element based validation of nonrigid registration using single- and multilevel free-form deformations: application to contrast-enhanced MR mammography. , 2002, 4684, 550.		4
133	Registration-based mesh construction technique for finite-element models of brains. , 2002, , .		4
134	On the Usage of GPUs for Efficient Motion Estimation in Medical Image Sequences. International Journal of Biomedical Imaging, 2011, 2011, 1-15.	3.9	4
135	Graph Cuts-Based Registration Revisited: A Novel Approach for Lung Image Registration Using Supervoxels and Image-Guided Filtering. , 2016, , .		4
136	Whole tumor kinetics analysis of 18F-fluoromisonidazole dynamic PET scans of non-small cell lung cancer patients, and correlations with perfusion CT blood flow. EJNMMI Research, 2018, 8, 73.	2.5	4
137	An Inverse Problem Approach to the Estimation of Volume Change. Lecture Notes in Computer Science, 2005, 8, 616-623.	1.3	4
138	Nonlinear Smoothing of MR Images Using Approximate Entropy — A Local Measure of Signal Intensity Irregularity. Lecture Notes in Computer Science, 1999, , 484-489.	1.3	4
139	A Clustering Method for the Extraction of Microcalcifications Using Epipolar Curves in Digital Breast Tomosynthesis. Lecture Notes in Computer Science, 2010, , 682-688.	1.3	4
140	Improving In Vivo High-Resolution CT Imaging of the Tumour Vasculature in Xenograft Mouse Models through Reduction of Motion and Bone-Streak Artefacts. PLoS ONE, 2015, 10, e0128537.	2.5	4
141	Simulation of Local and Global Atrophy in Alzheimer's Disease Studies. Lecture Notes in Computer Science, 2006, 9, 937-945.	1.3	4
142	Complete Fetal Head Compounding from Multi-view 3D Ultrasound. Lecture Notes in Computer Science, 2019, , 384-392.	1.3	4
143	PRETUS: A plug-in based platform for real-time ultrasound imaging research. SoftwareX, 2022, 17, 100959.	2.6	4
144	Improved 3D tumour definition and quantification of uptake in simulated lung tumours using deep learning. Physics in Medicine and Biology, 2022, , .	3.0	4

#	Article	IF	CITATIONS
145	Joint estimation of subject motion and tracer kinetic parameters of dynamic PET data in an EM framework. , 2012, , .		3
146	Multiview Machine Learning Using anÂAtlas of Cardiac Cycle Motion. Lecture Notes in Computer Science, 2018, , 3-11.	1.3	3
147	Correlating Tumour Histology and ex vivo MRI Using Dense Modality-Independent Patch-Based Descriptors. Lecture Notes in Computer Science, 2015, , 137-145.	1.3	3
148	Microcalcification Detection in Digital Breast Tomosynthesis Using an Epipolar Curve Approach. Lecture Notes in Computer Science, 2010, , 704-711.	1.3	3
149	A Generalised Spatio-Temporal Registration Framework for Dynamic PET Data: Application to Neuroreceptor Imaging. Lecture Notes in Computer Science, 2013, 16, 211-218.	1.3	3
150	Fusion of rat brain histology and MRI using weighted multi-image mutual information. , 2008, , .		2
151	The reconstruction of microcalcification clusters in digital breast tomosynthesis. , 2010, , .		2
152	Realistic biomechanical model of a cancerous breast for the registration of prone to supine deformations. , 2013, 2013, 7249-52.		2
153	Filling Large Discontinuities in 3D Vascular Networks Using Skeleton- and Intensity-Based Information. Lecture Notes in Computer Science, 2015, , 157-164.	1.3	2
154	Regression analysis for assessment of myelination status in preterm brains with magnetic resonance imaging. , 2016, , .		2
155	Non-local Graph-Based Regularization forÂDeformable Image Registration. Lecture Notes in Computer Science, 2017, , 199-207.	1.3	2
156	EchoFusion: Tracking and Reconstruction of Objects in 4D Freehand Ultrasound Imaging Without External Trackers. Lecture Notes in Computer Science, 2018, , 117-127.	1.3	2
157	Fast Groupwise 4D Deformable Image Registration for Irregular Breathing Motion Estimation. Lecture Notes in Computer Science, 2018, , 37-46.	1.3	2
158	Towards More Realistic Biomechanical Modelling of Tumours under Mammographic Compressions. Lecture Notes in Computer Science, 2010, , 481-489.	1.3	2
159	The Impact of Heterogeneity and Uncertainty on Prediction of Response to Therapy Using Dynamic MRI Data. Lecture Notes in Computer Science, 2013, 16, 316-323.	1.3	2
160	Spatial-temporal Pharmacokinetic Model Based Registration of 4D Brain PET Data. Lecture Notes in Computer Science, 2012, , 100-112.	1.3	2
161	Iteration-Dependent Networks and Losses for Unrolled Deep Learned FBSEM PET Image Reconstruction. , 2020, , .		2
162	A Biomechanical model of spiculated tumours under mammographic compressions. , 2010, 2010, 712-5.		1

0

#	Article	IF	CITATIONS
163	Towards 3D registration of fetal brain MRI and ultrasound. , 2012, , .		1
164	A probabilistic non-rigid registration framework using local noise estimates. , 2012, , .		1
165	pCT derived arterial input function for improved pharmacokinetic analysis of longitudinal dceMRI for colorectal cancer. Proceedings of SPIE, 2013, , .	0.8	1
166	A DCE-MRI imaging-based model for simulation of vascular tumour growth. , 2016, 2016, 5949-5952.		1
167	Hessian-assisted supervoxel: structure-oriented voxel clustering and application to mediastinal lymph node detection from CT volumes. Proceedings of SPIE, 2017, , .	0.8	1
168	Clinical feasibility of texture analysis in DCE MRI of patients receiving selective internal radiation therapy. European Journal of Surgical Oncology, 2018, 44, S30-S31.	1.0	1
169	Special issue on MICCAI 2018. Medical Image Analysis, 2019, 58, 101560.	11.6	1
170	Image-Based Artefact Removal in Laser Scanning Microscopy. IEEE Transactions on Biomedical Engineering, 2020, 67, 79-87.	4.2	1
171	Guest Editorial: Deep Learning in Ultrasound Imaging. IEEE Journal of Biomedical and Health Informatics, 2020, 24, 929-930.	6.3	1
172	Automatic Re-orientation of 3D Echocardiographic Images in Virtual Reality Using Deep Learning. Lecture Notes in Computer Science, 2021, , 177-188.	1.3	1
173	Deep Generative Models to Simulate 2D Patient-Specific Ultrasound Images in Real Time. Communications in Computer and Information Science, 2020, , 423-435.	0.5	1
174	An MRF-Based Discrete Optimization Framework for Combined DCE-MRI Motion Correction and Pharmacokinetic Parameter Estimation. Lecture Notes in Computer Science, 2014, , 73-84.	1.3	1
175	Oral nelfinavir before and during radiation therapy for rectal cancer: Changes in tumor perfusion and correlation between tissue and radiological markers of response Journal of Clinical Oncology, 2014, 32, 491-491.	1.6	1
176	Motion Correction of Intravital Microscopy of Preclinical Lung Tumour Imaging Using Multichannel Structural Image Descriptor. Lecture Notes in Computer Science, 2014, , 164-173.	1.3	1
177	Regional lung ventilation estimation based on supervoxel tracking. , 2018, , .		1
178	Elastic registration of chest CT images with log un-biased deformations and rigidity constraint. , 2011, , .		0
179	Biomedical Cancer Imaging Analysis. , 2012, , .		0

180 Tumor Growth Estimation via Registration of DCE-MRI Derived Tumor Specific Descriptors. , 2016, , .

#	Article	IF	CITATIONS
181	Editorial for the special issue of "Computational methods for molecular imaging―for computerized medical imaging and graphics. Computerized Medical Imaging and Graphics, 2017, 60, 1-2.	5.8	Ο
182	IJCARS-MICCAI 2018 special issue. International Journal of Computer Assisted Radiology and Surgery, 2019, 14, 1461-1461.	2.8	0
183	Mechanically Powered Motion Imaging Phantoms: Proof of Concept. , 2019, 2019, 2723-2726.		Ο
184	A Semi-automated Toolkit for Analysis of Liver Cancer Treatment Response Using Perfusion CT. Lecture Notes in Computer Science, 2014, , 23-32.	1.3	0
185	Mass Transportation for Deformable Image Registration with Application to Lung CT. Lecture Notes in Computer Science, 2017, , 66-74.	1.3	Ο
186	XeMRI to CT Lung Image Registration Enhanced with Personalized 4DCT-Derived Motion Model. Lecture Notes in Computer Science, 2018, , 260-271.	1.3	0
187	15â€Automatic mis-triggering artefact detection for image quality assessment of cardiac MRI. , 2018, , .		0
188	Learning Associations Between Clinical Information and Motion-Based Descriptors Using a Large Scale MR-derived Cardiac Motion Atlas. Lecture Notes in Computer Science, 2019, , 94-102.	1.3	0